

Dalton Transactions

Accepted Manuscript



This is an *Accepted Manuscript*, which has been through the Royal Society of Chemistry peer review process and has been accepted for publication.

Accepted Manuscripts are published online shortly after acceptance, before technical editing, formatting and proof reading. Using this free service, authors can make their results available to the community, in citable form, before we publish the edited article. We will replace this *Accepted Manuscript* with the edited and formatted *Advance Article* as soon as it is available.

You can find more information about *Accepted Manuscripts* in the [Information for Authors](#).

Please note that technical editing may introduce minor changes to the text and/or graphics, which may alter content. The journal's standard [Terms & Conditions](#) and the [Ethical guidelines](#) still apply. In no event shall the Royal Society of Chemistry be held responsible for any errors or omissions in this *Accepted Manuscript* or any consequences arising from the use of any information it contains.

ARTICLE

Three new solvent-directed Cd(II)-based MOFs with unique luminescent properties and highly selective sensor for Cu²⁺ cations and nitrobenzene†

Cite this: DOI: 10.1039/x0xx00000x

Received 00th January 2012,
Accepted 00th January 2012

DOI: 10.1039/x0xx00000x

www.rsc.org/

Yunlong Wu, Guo-Ping Yang*, Yanqing Zhao, Wei-Ping Wu, Bo Liu, Yao-Yu Wang*

Three new solvent-induced metal-organic frameworks (MOFs), [Cd(H₂L)(H₂O)₃]·NMP (**1**), [Cd₃(L)(H₂O)₄(OH)₂] (**2**) and [Cd(L)_{0.5}(H₂O)₂]·H₂O (**3**), have been rationally designed and successfully prepared via solvothermal reaction by the multidentate phenyltetracarboxylic acid [1,1':4',1''-terphenyl]-2',3,3'',5'-tetracarboxylic acid (H₄L) and Cd(II) salts in different solvent systems. The structural analyses indicate that the H₂L/L ligands took three different coordination fashions in **1–3** and thus resulted in the diversities of targeted MOFs. The solid state luminescent properties of three MOFs were studied under the irradiation of ultraviolet light at ambient temperature, especially for **3** showing a high selectivity and sensitivity for Cu²⁺ ions and nitrobenzene because of the quenching effect, which thus could make it be a potential crystalline material for detecting these substances. There are also discussions of the mechanism of quenching effect and sensing properties of **3** in detail.

Introduction

Nowadays, it is well known that the environmental problems are becoming more and more serious in our daily life and even have a lethal influence on the living organisms. Therefore, a great deal of funds and attention has been urgently flowed to these issues, particularly for the toxic organic substances and heavy metal ions.¹ Among these poisonous substances, there is a great demand for the nitro aromatic complexes, especially for nitrobenzene (NB) as the broadly raw materials in the chemical synthesis of the pesticides and explosives.² However, NB is a highly serious toxic pollutant, the excessive ingestion of which may cause some diseases, such as the vomiting and coma et al.³ Similarly, the heavy metal ions, particularly for Cu²⁺ cations, are also essential to the smelting industries and humans. Of course, the excessive intake of Cu²⁺ ions might contribute to the health problems, such as the Alzheimer and Parkinson's disease, amyotrophic lateral sclerosis et al.⁴ Thereby, how to monitor the NB and Cu²⁺ ions quickly and effectively is becoming a hot spot for the chemists.⁵

At present, there are kinds of the sophisticated commercial methods to detect these contaminants, the applications of which are, however, of great limitation for the shortcomings, i.e. low portability, complex pretreatments, and expensive instruments et al. Fortunately, the recent studies show that the fluorimetric method based on the luminescent metal-organic frameworks (MOFs) as the probes have the unique advantages, such as the nondestructive detection, high sensitivity, fast response, and real-time monitor. More importantly, the structures of MOFs

can usually be fine-tuned by incorporation of functional groups and reaction conditions to improve their emission properties.⁶ As a key factor, solvent is an essential component for reactions in solution and therefore plays a significant role in the assembly process of targeted MOFs. Recently, Du et al reviewed the role of different solvents in various reaction systems, including crystal growth, structural regulation, transformations and so on,⁷ which may supply some new insights to the predesign and construction of such materials. Our group has also reported several interesting solvent-induced MOFs in recent works,⁸ and the results indicate the networks of MOFs are mainly directed by the solvent size and polarity. Although much effort has already been devoted in this aspect by accident or predesign, the mechanism of the solvent effect is still largely unexplored and out of control, and there thus remains a lot of research work to improve and perfect this current situation.

As an effective combination of the above stated aspects and our previous research works, our group herein report three new solvent-directed Cd(II)-MOFs, i.e. [Cd(H₂L)(H₂O)₃]·NMP (**1**), [Cd₃(L)(OH)₂(H₂O)₄] (**2**), and [Cd(L)_{0.5}(H₂O)₂]·H₂O (**3**), based on a multidentate tetracarboxylic acid [1,1':4',1''-terphenyl]-2',3,3'',5'-tetracarboxylic acid (H₄L) in different solvent systems. The structural analyses show that the H₂L/L ligands take three different coordination fashions in three MOFs and thus resulted in diversities of MOFs. The solid state luminescent properties have also been conducted under the irradiation of ultraviolet at ambient temperature, especially for **3** showing a high selectivity and sensitivity for Cu²⁺ ions and NB because of the quenching effect, which therefore may be a

potential material for detecting these substances. There are also discussions of the mechanism of quenching effect and sensing properties of **3**.

Experimental section

Materials and general methods

All starting materials and reagents used in the experiment were commercially available and of analytical grade without further purification. The infrared spectra were acquired by a BRUKER EQUINOX-55 FT-IR spectrometer with KBr discs in 4000 ~ 400 cm^{-1} . Elemental analyses (C, H and N) were measured by a Perkin-Elmer 2400C elemental analyzer. Thermogravimetric analyses (TGA) were collected by using the NETZSCH STA 449C microanalyzer thermal analyzer from 25 ~ 800 $^{\circ}\text{C}$ under the protection of N_2 . Powder X-ray diffraction (PXRD) patterns were carried out by a Bruker D8 ADVANCE X-ray powder diffractometer (Cu-K α , $\lambda = 1.5418 \text{ \AA}$) with the 2θ from 5 ~ 50 $^{\circ}$ under the 0.03 $^{\circ}$ scan step. The solid state luminescent spectra and the emissive lifetimes were recorded by the Hitachi F4500 and the Flsp920 fluorescence spectrophotometer at ambient temperature, respectively.

Synthesis of $[\text{Cd}(\text{H}_2\text{L})(\text{H}_2\text{O})_3]\cdot\text{NMP}$ (**1**)

A mixture of $\text{Cd}(\text{NO}_3)_2\cdot 6\text{H}_2\text{O}$ (0.1 mmol, 30.8 mg), H_4L (0.05 mmol, 20.3 mg), NaOH (0.1 mL, 1 mol/L) and NMP/ H_2O (4 mL/6 mL) was sealed in a 15 mL Teflon lined stainless steel vessel, which then heated at 145 $^{\circ}\text{C}$ for 72 h and cooled to 25 $^{\circ}\text{C}$ with a rate of 0.5 $^{\circ}\text{C}/\text{min}$. As a result, the colorless prism crystals were obtained, washed by NMP- H_2O and then dried in the air. Yield 52% based on H_4L . Elemental analysis of **1**, calcd (%): C 48.41, H 4.06, N 2.09; found: C 48.29, H 4.2, N 2.21. FT-IR (KBr, cm^{-1}) (Fig. S1, ESI †): 3136 (s), 2511 (m), 1663 (s), 1554 (s), 1476 (s), 1351 (s), 1178 (m), 1053 (m), 922 (m), 873 (m), 840 (m), 759 (s), 680 (s), 582 (m).

Synthesis of $[\text{Cd}_3(\text{L})(\text{OH})_2(\text{H}_2\text{O})_4]$ (**2**)

Similar to that of **1**, except that DMF instead of NMP (4 mL) in the synthesis process, the colorless needle-like crystals of **2** were isolated. Yield: 48% (based on H_4L). Elemental analysis of **2**, calcd (%): C 31.25, H 2.38; found: C 31.43, H 2.47. FT-IR (KBr, cm^{-1}): 3425 (s), 1566 (s), 1468 (s), 1136 (m), 1088 (m), 908 (s), 835 (s), 798 (s), 761 (s), 700 (s), 676 (s), 627 (s), 553 (s), 443 (s).

Synthesis of $[\text{Cd}(\text{L})_{0.5}(\text{H}_2\text{O})]\cdot\text{H}_2\text{O}$ (**3**)

Using the same raw materials of **1** and **2**, the crystalline products of **3** were successfully formed in the different mixed solvent DMA/ H_2O (4 mL/6 mL). Yield: 61% (based on H_4L). Elemental analysis for **3**, calcd (%): C 37.79, H 2.59; found: C 37.83, H 2.61. FT-IR (KBr, cm^{-1}): 3410 (s), 1548 (s), 1407 (s), 1260 (s), 1084 (m), 1016 (w), 918 (w), 889 (m), 849 (s), 771 (s), 683 (s), 585 (s), 543 (m), 485 (m), 416 (m).

Crystal Structure Determinations

Suitable single crystals of **1–3** were tested on a Bruker SMART APEXII CCD diffractometer equipped with a graphite-monochromated Mo-K α radiation ($\lambda = 0.71073 \text{ \AA}$) at room temperature. The structures were solved by the direct methods and refined by a full-matrix least-squares refinement on F^2 with SHELXL-97 and SHELXS-97.⁹ The hydrogen atoms were

calculated and assigned their ideal positions with the isotropic displacement factors and included in the final refinement by use of geometrical restraints. The relevant crystallographic data are summarized in Table 1. Selected bond lengths and angles are listed in Table S1 (ESI †). CCDC Nos. 1032234–1032236 for MOFs **1–3**.

Table 1. Crystal data and structure refinements for **1–3**.

Compound	1	2	3
Formula	$\text{C}_{27}\text{H}_{27}\text{CdNO}_{12}$	$\text{C}_{22}\text{H}_{20}\text{Cd}_3\text{O}_{14}$	$\text{C}_{11}\text{H}_9\text{CdO}_6$
Formula mass	669.90	845.58	349.59
Crystal system	Orthorhombic	Monoclinic	Tetragonal
Space group	<i>Pnma</i>	<i>P2₁/c</i>	<i>I4₁/a</i>
<i>a</i> [\AA]	11.4313(19)	11.0483(18)	18.1586(14)
<i>b</i> [\AA]	17.928(3)	6.6820(11)	18.1586(14)
<i>c</i> [\AA]	12.983(2)	17.638(3)	14.416(2)
α [$^{\circ}$]	90	90	90
β [$^{\circ}$]	90	107.833(2)	90
γ [$^{\circ}$]	90	90	90
<i>V</i> [\AA^3]	2660.8(8)	1239.6(4)	4753.4(9)
<i>Z</i>	4	2	16
<i>D</i> _{calcd} [$\text{g}\cdot\text{cm}^{-3}$]	1.672	2.266	1.954
μ [mm^{-1}]	0.889	2.624	1.854
<i>F</i> [000]	1360	816	2736
θ [$^{\circ}$]	1.94–25.00	1.94–25.09	1.80–25.08
Reflections collected	12519/2423	5881/2201	11566/2105
GOOF	1.003	1.057	1.038
<i>R</i> ^[a] [$I > 2\sigma(I)$]	<i>R</i> ₁ = 0.0415 <i>wR</i> ₂ = 0.1242	<i>R</i> ₁ = 0.0290 <i>wR</i> ₂ = 0.0841	<i>R</i> ₁ = 0.0283 <i>wR</i> ₂ = 0.0986
^a $R_1 = \sum F_o - F_c / \sum F_o $, $wR_2 = [\sum w(F_o^2 - F_c^2)^2 / \sum w(F_o^2)^2]^{1/2}$			

Results and discussion

Structure description of $[\text{Cd}(\text{H}_2\text{L})(\text{H}_2\text{O})_3]\cdot\text{NMP}$ (**1**)

Single-crystal X-ray analysis reveals that compound **1** crystallizes in the orthorhombic *Pnma* space group, and the asymmetry unit consists of one partly deprotonated H_2L^{2-} ligand, three coordination water and one disordered NMP molecule. Each Cd(II) ion is seven-coordinated by seven oxygen atoms which involve four oxygen atoms from two H_2L ligands and three oxygen atoms from three water molecules, as shown in Fig. 1a. And all the Cd–O bond lengths [2.274(2) ~ 2.5649(14) \AA] and Cd–O–Cd angles [52.50(4) $^{\circ}$ ~ 177.98(5) $^{\circ}$] fall into the normal range of the other reported Cd(II)-based carboxylate complexes.¹⁰

In **1**, there are two uncoordinated carboxylic groups of H_2L ligand which are protonated to balance the charge with Cd(II) ions, and thus, the H_2L ligand adopts a bidentate coordination model ($\eta^2\mu_1\chi^2$), as depicted in Scheme 1a. Each H_2L ligand alternately links two different Cd(II) ions to generate an infinite 1D zigzag-like chain structure (Fig. 1b). Due to the existence of the large number of protonated carboxylic groups and water molecules, there are abundant of hydrogen bonds in **1**. The adjacent 1D chains interlock each other to give a 2D infinite

layer via hydrogen bonds of O3–H···O2 and O5–H···O4 (O···O, 2.622 and 2.885 Å, Fig. S2, ESI†). Then a 3D supramolecular framework of **1** is further condensed from these 2D layers via the additional hydrogen bonds, where the guest NMP molecules are located in the 1D porous channels (Fig. 1c).

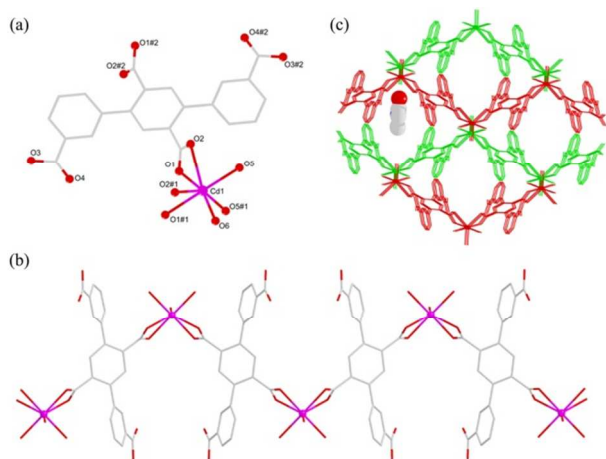
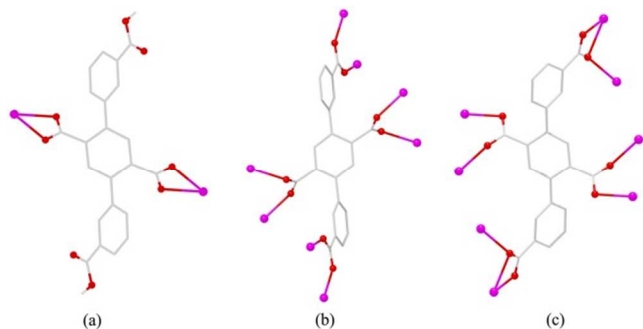


Fig. 1 (a) The view of the coordination environment of Cd(II) center in **1**, symmetry codes: #1: $x, -y+1.5, z$; #2: $-x, -y+2, -z+2$. (b) The 1D zigzag-like chain structure. (c) The perspective view of the 3D supramolecular structure of **1** via a axis.



Scheme 1 The various coordination fashions of the H_2L/L ligands with Cd(II) cations.

Structure description of $[Cd_3(L)(OH)_2(H_2O)_4]$ (**2**)

Compound **2** crystallizes in the monoclinic $P2_1/c$ space group, showing a 3D non-interpenetrated framework constructed by 1D rod-like SBUs and L ligands. The fundamental unit includes three independent Cd(II) ions (Cd1, 2Cd2), one L ligand, two hydroxyls and four water molecules. All the Cd(II) ions adopt the distorted octahedral geometries formed by six oxygen atoms. As illustrated in Fig. 2a, Cd1 is coordinated by four oxygen atoms from four different L ligands and two oxygen atoms from two hydroxyls, while Cd2 takes coordination with two oxygen atoms from two L ligands, two water molecules and two hydroxyls. The distances of Cd–O bonds range from 2.227(3) to 2.382(3) Å, and the bond angles around the Cd(II) centers are in the range of 77.41(12)–180.00(12)°. The four carboxylate groups of L ligands in **2** adopt the bridging bidentate ($\eta^2\mu_2\chi^2$) connection fashion with Cd(II) ions (Scheme 1b).

In **2**, an infinite 1D rod-like SBU is formed by Cd(II) ions, hydroxyls and carboxylate groups of L ligands along the c axis, where one Cd1 and two Cd2 atoms alternately link each other

to result in the metal sequence $\cdots Cd1 \cdots 2Cd2 \cdots$ (Fig. 2b). Then these neighboring SBUs are further supported via the L ligands to produce a dense 3D framework (Fig. 2c), the holes of which are encapsulated by the coordinated water molecules, therefore, there are no additionally residual solvent accessible voids of the unit cell of **2** by the estimation by the PLATON program.¹¹ For more clear and simple analysis of the complicated 3D network, the topological approach is adapted to simplify the framework. Herein, the carbon atoms of the carboxylate in the SBU can be considered as the extended nodes, and these SBUs can thus be simplified as the 1D zigzag linkers. Then, when the L ligands acting as 4-connected nodes, the framework of **2** thereby shows a binodal (4,6)-connected topological net (Fig. 2d) with the point symbol $(5^{10}.6^3.7^8)(5^4.6^2)$, as far as we know, which has scarcely been observed in 3D MOFs based on the 1D infinite rod-shaped SBUs.¹²

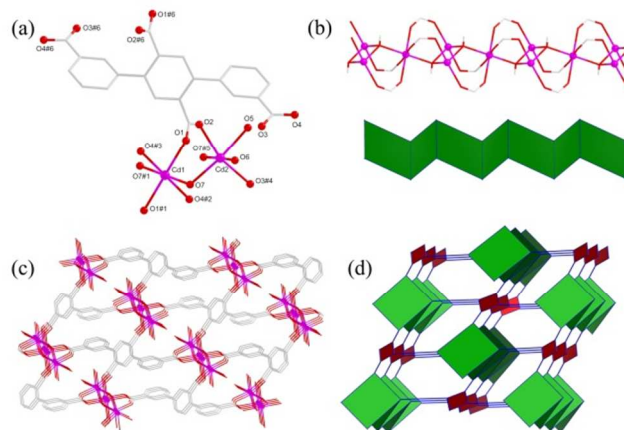


Fig. 2 (a) The coordination environment of Cd(II) ions in **2**, symmetry codes: #1: $1-x, -y, -z$; #2: $1-x, y-0.5, 0.5-z$; #3: $x, 0.5-y, z-0.5$; #4: $1-x, 0.5+y, 0.5-z$; #5: $1-x, 1-y, -z$; #6: $-x, -y, -z$. (b) The 1D rod-like SBU formed by Cd(II) ions, hydroxyls and carboxylate groups of L ligands (top) and its simplified net (below). (c) The 3D dense framework of **2**. (d) The topological net of **2**.

Structure description of $[Cd(L)_{0.5}(H_2O)_2] \cdot H_2O$ (**3**)

Different from compounds **1** and **2**, X-ray diffraction analysis reveals that compound **3** crystallizes in the tetragonal $I4_1/a$ space group. As shown in Fig. 3, the asymmetry unit consists of one Cd(II) cation, half of one deprotonated L ligand, two coordinated water molecules and one lattice water molecule. The Cd(II) atom is coordinated by six oxygen atoms to produce the distorted octahedral geometry, where the oxygen atoms come from four different L ligands and one coordinated water. The carboxylates of L ligands in **3** take coordination with Cd(II) ions by two distinct modes: the bridging bidentate ($\eta^2\mu_2\chi^2$) and tridentate ($\eta^3\mu_2\chi^3$) coordination fashions (Scheme 1c).

There is an infinite 1D Cd(II)-carboxylate cluster as the basic SBU running along the c axis in **3** (Fig. 4a), which is similar to the structural feature of **2**. Furthermore, each chain is connected with four neighboring ones by L ligands along the a and b axis to isolate the 3D framework (Fig. 4b). Notably, it is found that a porous cage can be constructed from the four rod SBUs connection with the eight distorted L units (Fig. 4c), and the guest water molecules are included in these micropores. The solvent accessible space of the crystal unit cell (4753.5 \AA^3) is calculated to be 293.1 \AA^3 (6.2%) by the PLATON program. While the 3D porous system of **3** possesses the large void volume of 1149.6 \AA^3 (24.2%) after excluding the lattice and

coordinated water molecules. Topologically, each Cd(II) ion connects four L units, and each L ligand links eight Cd(II) centers, so they are simplified as 4- and 8-nodes, respectively. Thereby, the framework of **3** is designated as a binodal (4,8)-connected net with the point symbol $(4^5.6)_2(4^{10}.6^2.8^{16})$, which represents a rarely topological network with the higher mixed nodes in 3D hybrid MOFs.¹³

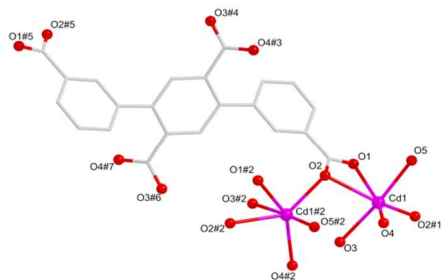


Fig. 3 The coordination environment of Cd(II) cations in **3**. Symmetry codes: #1: $y+0.25, -x+0.25, z+0.25$; #2: $-y+0.25, x-0.25, z-0.25$; #3: $-y-0.25, x-0.25, -z+1.75$; #4: $x-0.5, y, -z+1.5$; #5: $-x, -y, -z+1$; #6: $-x+0.5, -y, z-0.5$; #7: $y+0.25, -x+0.25, z-0.75$.

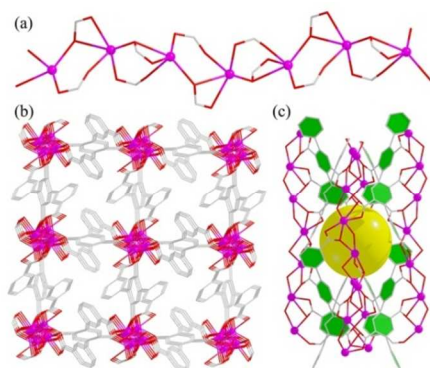


Fig. 4 (a) The perspective view of 1D Cd(II)-carboxylate cluster. (b) The 3D packing pattern of **3**. (c) The porous cage built by the four SBUs with eight distorted L units.

Role of the solvents in the assembly of MOFs 1–3

It has been proven that some prime factors, including the solvent, pH value, molar ratio of the reactants and reaction temperature etc, can govern and mediate the assembly process of MOFs.¹⁴ In this work, three MOFs have been successfully synthesized by using the same initial reactants but in different mixed H₂O/carbonyl solvent systems (NMP for **1**, DMF for **2**, and DMA solution for **3**, respectively). From what has been discussed above, three MOFs represent the different structural frameworks based on the various linkages of L ligands and Cd(II) ions, especially the partially protonated H₂L ligands in **1**. The water molecules took coordination with Cd(II) ions as the terminated ligands in three MOFs, however, there are also some drastic differences among the architectures of MOFs. Firstly, there are free NMP molecules in the crystalline host lattice of **1**. While the hydroxyl group is involved in coordination and balance the charges with Cd(II) cations in **2**. Furthermore, some parallel experiments were carried out under the same synthesis conditions and solvent ratio by employment of various solvents, such as methanol and ethanol et al, where no suitable crystals

were obtained. Obviously, the assemblies of the MOFs are very sensitive to the carbonyl solvent in this reaction system.

PXRD and the thermogravimetric analyses

The powder X-ray diffraction (PXRD) experiments of three MOFs were carried out carefully to check the phase purity at room temperature. The patterns show that the main peaks of the synthesized MOFs are closely consistent with those of the simulated from the single crystal X-ray diffraction data, which imply the high qualities of the obtained products (Fig. S3, ESI†). Moreover, the thermal stabilities of MOFs **1–3** have also been detected by the thermogravimetric analysis (TGA) (Fig. S4, ESI†). The TGA curves of three MOFs show that the frameworks have the similar thermal stabilities. They all firstly lose the coordination water molecules and hydroxyl groups or lattice molecules, after that they can keep their host frameworks at the lower temperatures, and then the structural skeletons begin to collapse beyond the stable temperatures.

Luminescence measurements and discussions

The luminescent MOFs with different d¹⁰ metal ions have been the potential candidates for their excellent photoactive materials.¹⁵ Thereby, the solid state luminescent properties of pure H₄L ligand and MOFs **1–3** were investigated carefully at room temperature, as displayed in Fig. 5. The maximum emission peaks of H₄L ligand and **1–3** are observed at ~414 nm for H₄L ligand ($\lambda_{\text{ex}} = 280$ nm), ~378 nm for **1** and **2** ($\lambda_{\text{ex}} = 300$ nm), ~414 nm for **3** ($\lambda_{\text{ex}} = 350$ nm), respectively. The emission spectra of **1** and **2** display the obvious blue shift compared to that of H₄L ligand, owing to the effect of the ligand-metal coordination interactions.¹⁶ The emission of **3** is very similar to that of H₄L ligand, which may arise from the ligand-centered $\pi-\pi^*$ electronic transitions compared with the reported luminescent d¹⁰ MOFs. In addition, the luminescent lifetimes have also been tested for the three MOFs, which are 4.1 ns, 3.6 ns, and 4.1 ns for **1–3**, respectively (Fig. S5, ESI†). Particularly, the products of **3** as the luminescent probes has been explored carefully for sensing the different metal ions and small solvent molecules, owing to its strong visible blue light when excited by the ultraviolet light (Fig. S6, ESI†).

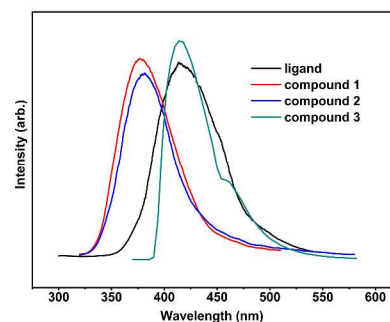


Fig. 5 The solid state emission spectra of H₄L ligands and MOFs **1–3**.

In order to study the luminescent responses of **3** to different metal ions, the products of **3** was grinded into the powder and suspended in DMA solution containing the same concentration of $M(\text{NO}_3)_n$ ($M = \text{Li}^+, \text{Na}^+, \text{K}^+, \text{Ag}^+, \text{Ca}^{2+}, \text{Mg}^{2+}, \text{Mn}^{2+}, \text{Pb}^{2+}, \text{Hg}^{2+}, \text{Zn}^{2+}, \text{Cd}^{2+}, \text{Co}^{2+}, \text{Ni}^{2+}, \text{Al}^{3+}, \text{and Cu}^{2+}$) for 24 hours. As depicted in Figs. 6a and 6b, the luminescent intensities of **3** are decreased sharply by Co^{2+} , Al^{3+} , and Ni^{2+} ions, particularly for Cu^{2+} ion, which has the excellent quenching effect to the system

as highly selective sensor (Fig. S7, ESI[†]). Also, the quantitative sensitizations of quenching behavior have also been examined via changing the concentration of Cu²⁺ cations in solution. The

More importantly, the relationships between the luminescent intensities of **3** and the concentration of Cu²⁺ cations or NB molecules could be in good agreement with the first-order

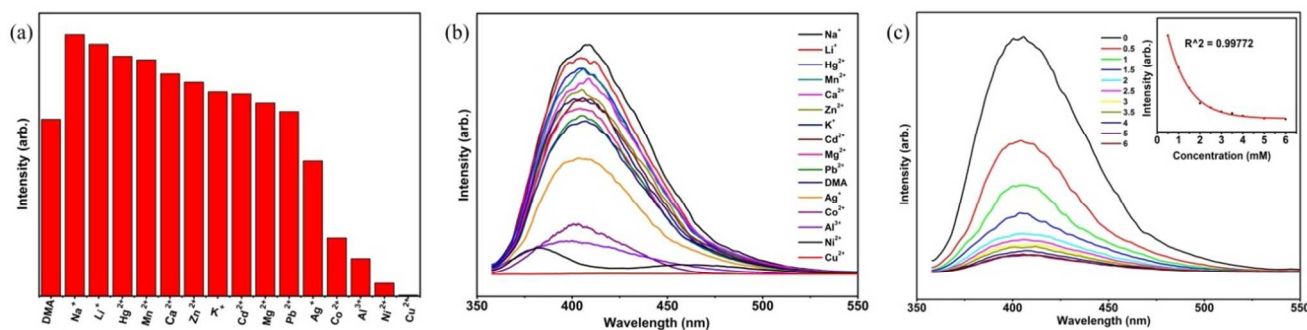


Fig. 6 (a) The comparisons of the luminescent intensities of **3** in different metal ions in DMA solution; (b) The emission spectra of **3** in different metal ions in DMA; (c) The different strength intensities of the luminescent spectra of **3** in DMA with different amounts of Cu²⁺ ions (Insert: the relationship of the luminescent intensities and Cu²⁺ concentration in DMA).

titration experiments indicate that the luminescent intensities are gradually weakened by increasing the amount of Cu²⁺ ions (Fig. 6c). The reason may be explained for that the out layers of Co²⁺, Ni²⁺, and Cu²⁺ ions have the unsaturated electronic state (d⁷, d⁸, and d⁹), which make the ions keep the empty orbits and thus become the ideal acceptors for electrons, while the rest of ions (Na⁺, K⁺, Cd²⁺, Hg²⁺, and Ag⁺), possessing the saturated state (p⁶, and d¹⁰), cannot accept additional electrons from other atoms.¹⁷ Thereby, the unique quenching behavior herein may mainly ascribe to the interactions of Cu²⁺ cations and oxygen atoms of carboxylates from L ligands in **3**, which cause the electrons of L ligands to transfer from **3** to Cu²⁺ ions as electron acceptors, thus inducing the above luminescent decay.

Moreover, the luminescent sensing for the different solvent molecules was also investigated carefully by immersing the crystalline powder of **3** in solvents for 24 hours. It is found that the luminescent intensities of **3** are dependent on the different solvents (Figs. 7a and 7b). More attractively, the luminescent intensity of **3** can be completely quenched by NB molecules compared to other solvents. Meanwhile, NB molecules was added slowly to the suspension of **3** in DMA solution to study the quantitative quenching effect of **3**, showing the distinctly gradual decrease of luminescent intensities (Fig. 7c). As known to all, nitro-group is a withdrawing electron substituent and can stabilize the lowest unoccupied molecular orbital (LUMO) of the aromatic products via the conjugation compared with other solvents, which might lead the electrons to transfer from the phenyl rings of L ligands of **3** to NB through the interactions of the framework of **3** and NB molecules.¹⁸

exponential equation (insert of Figs. 6c and 7c), displaying the diffusion-controlled quenching process for the Cu²⁺ ions or NB molecules.¹⁹ These excellent results indicate that the crystalline products of **3** can be used as the excellent luminescent sensor to detect Cu²⁺ ions and NB as the highly selective luminescent crystalline materials.

Conclusions

In summary, three new solvent-directed Cd(II)-MOFs have been solvothermally synthesized in different solvent systems. It is found that the H₂L/L ligands displays three different coordination fashions in the obtained MOFs and thus give rise to the various structural diversities of MOFs. The solid state luminescent properties of three products have been studied via ultraviolet light at room temperature, especially for **3** showing the highly selective sensitivity for Cu²⁺ ions and NB molecules, which can be used as the potential material for detecting these poisonous substances. There are also further discussions of the mechanism of quenching effect and sensing properties of **3**. This work provides an easy and facile route to design and yield the new luminescent MOFs as promising functional materials, and the further research works about the sensing materials are underway in our group.

Acknowledgements

This work was supported by the NSFC (Grants 21201139, and

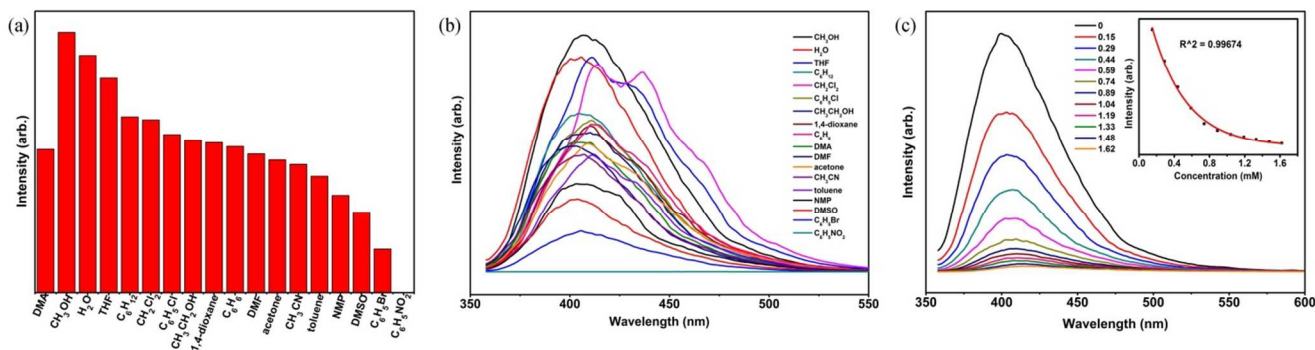


Fig. 7 (a) The relative luminescent intensities of **3** in different solvents; (b) The emission spectra of **3** in different solvents; (c) The luminescent spectra of **3** in DMA with different amounts of NB (Insert: the relationship of the luminescent intensities and NB concentration).

21371142), NSF of Shaanxi Province (Grant 2013JQ2016), and the Open Foundation of Key Laboratory of Synthetic and Natural Functional Molecule Chemistry of Ministry of Education (Grant 338080049).

Notes and references

Key Laboratory of Synthetic and Natural Functional Molecule Chemistry of Ministry of Education, Shaanxi Key Laboratory of Physico-Inorganic Chemistry, College of Chemistry and Materials Science, Northwest University, Xi'an 710069, P.R. China. E-mail: ygp@nwu.edu.cn, wyaoyu@nwu.edu.cn.

† Electronic Supplementary Information (ESI) available: TGA and PXRD patterns, and additional figures of MOFs. For ESI and crystallographic data in CIF or other electronic format. See DOI: 10.1039/b000000x/

- (a) E. Barea, C. Montoro and J. A. R. Navarro, *Chem.Soc.Rev.*, 2014, **43**, 5419; (b) X.-Z. Song, S.-Y. Song, S.-N. Zhao, Z.-M. Hao, M. Zhu, X. Meng, L.-L. Wu and H.-J. Zhang, *Adv. Funct. Mater.*, 2014, **24**, 4034; (c) J.-M. Zhou, W. Shi, H.-M. Li, H. Li and P. Cheng, *J. Phys. Chem. C*, 2014, **118**, 416; (d) J.-M. Zhou, W. Shi, N. Xu and P. Cheng, *Inorg. Chem.*, 2013, **52**, 8082; (e) M. E. Germain and M. J. Knapp, *Chem. Soc. Rev.*, 2009, **38**, 2543.
- (a) Z.-C. Hu, B. J. Deibert and J. Li, *Chem.Soc.Rev.*, 2014, **43**, 5815; (b) A.-J. Lan, K.-H. Li, H.-H. Wu, D. H. Olson, T. J. Emge, W. Ki, M.-C. Hong and J. Li, *Angew. Chem., Int. Ed.*, 2009, **48**, 2334; (c) G.-Y. W, C. Song, D.-M. Kong, W.-J. Ruan, Z. Chang and Y. Li, *J. Mater. Chem. A.*, 2014, **2**, 2213; (d) B. Gole, A. K. Bar and P. S. Mukherjee, *Chem. Eur. J.*, 2014, **20**, 2276.
- (a) D. Tian, Y. Li, R.-Y. Chen, Z. Chang, G.-Y. Wang and X.-H. Bu, *J. Mater. Chem. A.*, 2014, **2**, 1465; (b) Z.-F. Wu, B. Tan, M.-L. Feng, A.-J. Lan and X.-Y. Huang, *J. Mater. Chem. A.*, 2014, **2**, 6426.
- E. Gaggelli, H. Kozłowski, D. Valensin and G. Valensin, *Chem.Rev.*, 2006, **106**, 1995.
- (a) L. E. Kreno, K. Leong, O. K. Farha, M. Allendorf, R. P. V. Duyne and J. T. Hupp, *Chem. Rev.*, 2012, **112**, 1105; (b) Y.-J. Cui, Y.-F. Yue, G.-D. Qian and B.-L. Chen, *Chem. Rev.*, 2012, **112**, 1126; (c) D.-X. Ma, B.-Y. Li, X.-J. Zhou, Q. Zhou, K. Liu, G. Zeng, G.-H. Li, Z. Shi and S.-H. Feng, *Chem. Commun.*, 2013, **49**, 8964; (d) Z.-M. Hao, X.-Z. Song, M. Zhu, X. Meng, S.-N. Zhao, S.-Q. Su, W.-T. Yang, S.-Y. Song and H.-J. Zhang, *J. Mater. Chem. A.*, 2013, **1**, 11043; (e) J.-S. Qin, S.-J. Bao, P. Li, W. Xie, D.-Y. Du, L. Zhao, Y.-Q. Lan and Z.-M. Su, *Chem. Asian J.*, 2014, **9**, 749; (f) L.-Y. Pang, G.-P. Yang, J.-C. Jin, M. Kang, A.-Y. Fu, Y.-Y. Wang and Q.-Z. Shi, *Cryst. Growth Des.*, 2014, **14**, 2954; (g) Z. Hao, G. Yang, X. Song, M. Zhu, X. Meng, S. Zhao, S. Song and H. Zhang, *J. Mater. Chem. A.*, 2014, **2**, 237; (h) W. Yang, J. Feng and H. Zhang, *J. Mater. Chem.*, 2012, **22**, 6819.
- (a) W.-W. Zhan, Q. Kuang, J.-Z. Zhou, X.-J. Kong, Z.-X. Xie and L.-S. Zheng, *J. Am. Chem. Soc.*, 2013, **135**, 1926; (b) J.-S. Costa, S. Rodríguez-Jiménez, G.-A. Craig, B. Barth, C. M. Beavers, S. J. Teat and G. Aromí, *J. Am. Chem. Soc.*, 2014, **136**, 3869; (c) R. Wang, X.-Y. Dong, H. Xu, R.-B. Pei, M.-L. Ma, S.-Q. Zang, H.-W. Hou and T. C. W. Mak, *Chem. Commun.*, 2014, **50**, 9153; (d) X.-Y. Dong, R. Wang, J.-Z. Wang, S.-Q. Zang and T. C. W. Mak, *J. Mater. Chem. A.*, 2015, doi: 10.1039/C4TA04421E; (e) L.-H. Cao, Y. Wei, C. Ji, M.-L. Ma, S. Q. Zang and T. C. W. Mak, *Chem. Asian J.*, 2014, **9**, 3094.
- (a) M. Du, X. G. Wang, Z.-H. Zhang, L. F. Tang and X. J. Zhao, *CrystEngComm*, 2006, **8**, 788; (b) C. P. Li and M. Du, *Chem. Commun.*, 2011, **47**, 5958.
- (a) J. Li, G. P. Yang, L. Hou, L. Cui, Y. P. Li, Y. Y. Wang and Q.-Z. Shi, *Dalton Trans.*, 2013, **42**, 13590; (b) X. Zhou, P. Liu, W. H. Huang, M. Kang, Y. Y. Wang and Q. Z. Shi, *CrystEngComm*, 2013, **15**, 8125; (c) W. H. Huang, G. P. Yang, J. Chen, X. Chen, C. P. Zhang, Y. Y. Wang and Q. Z. Shi, *Cryst. Growth Des.*, 2013, **13**, 66.
- (a) G. M. Sheldrick, SHELXL-97, *Program for Refinement of Crystal Structures*, University of Göttingen, Germany, 1997; (b) V. A. Blatov, M. O'Keeffe, D. M. Proserpio, *CrystEngComm*, 2010, **12**, 44.
- (a) S.-S. Chen, P. Wang, S. Takamizawa, T.-A. Okamura, M. Chen and W.-Y. Sun, *Dalton Trans.*, 2014, **43**, 6012; (b) L.-P. Xue, X.-H. Chang, S.-H. Li, L.-F. Ma and L.-Y. Wang, *Dalton Trans.*, 2014, **43**, 7219; (c) L. Luo, K. Chen, Q. Liu, Y. Lu, T.-A. Okamura, G.-C. Lv, Y. Zhao and W.-Y. Sun, *Cryst. Growth Des.*, 2013, **13**, 2312; (d) J.-C. Jin, N.-N. Yan, W.-G. Chang, J.-Q. Liu, Z.-C. Yin, G.-N. Xu, K.-F. Yue, Y.-Y. Wang, *J. Coord. Chem.*, 2013, **66**, 3509.
- (a) A. L. Spek, *PLATON-A multipurpose Crystallographic Tool*, Utrecht University, Utrecht, The Netherlands, 2004; (b) L. Spek, *PLATON*, The University of Utrecht, Utrecht, The Netherlands, 1999.
- N. L. Rosi, J. Kim, M. Eddaoudi, B.-L. Chen, M. O'Keeffe and O. M. Yaghi, *J. Am. Chem. Soc.*, 2005, **127**, 1504.
- (a) R. Natarajan, G. Savitha, P. Dominiak, K. Wozniak, J. N. Moorthy, *Angew. Chem., Int. Ed.*, 2005, **44**, 2115; (b) M. Du, Z. H. Zhang, X. J. Zhao, Q. Xu, *Inorg. Chem.*, 2006, **45**, 5785; (c) M. Du, Z. H. Zhang, L. F. Tang, X. G. Wang, X. J. Zhao, S. R. Batten, *Chem. Eur. J.*, 2007, **13**, 2578.
- (a) M. W. Zhang, M. Bosch, T. Gentle III, H. C. Zhou, *CrystEngComm*, 2014, **16**, 4069; (b) G. P. Yang, L. Hou, L. F. Ma and Y. Y. Wang, *CrystEngComm*, 2013, **15**, 2561; (c) C. Huang, F. X. Ji, L. Liu, N. Li, H. F. Li, J. Wu, H. W. Hou and Y. T. Fan, *CrystEngComm*, 2014, **16**, 2615.
- (a) Y. Yu, X.-M. Zhang, J.-P. Ma, Q.-K. Liu, P. Wang and Y.-B. Dong, *Chem. Commun.*, 2014, **50**, 1444; (b) W.-L. Tong, S.-M. Yiu and M. C. W. Chan, *Inorg. Chem.*, 2013, **52**, 7114; (c) X.-H. Jin, J.-K. Sun, L.-X. Cai and J. Zhang, *Chem. Commun.*, 2011, **47**, 2667; (d) B. Gole, A. K. Bar and P. S. Mukherjee, *Chem. Commun.*, 2011, **47**, 12137; (e) L. Sun, H.-Z. Xing, J. Xu, Z.-Q. Liang, J.-H. Yu and R.-R. Xu, *Dalton Trans.*, 2013, **42**, 5508.
- (a) L. F. Ma, Q. L. Meng, C. P. Li, B. Li, L. Y. Wang, M. Du and F. P. Liang, *Cryst. Growth Des.*, 2010, **10**, 3036; (b) F.-F. Li, J.-F. Ma, S.-Y. Song, J. Yang, Y.-Y. Liu and Z.-M. Su, *Inorg. Chem.*, 2005, **44**, 9374.
- (a) K. Jayaramulu, R. P. Narayanan, S. J. George and T. K. Maji, *Inorg. Chem.*, 2012, **51**, 10089; (b) B. L. Chen, L. B. Wang, Y. Q. Xiao, Frank R. Fronczek, M. Xue, Y. J. Cui and G. D. Qian, *Angew. Chem., Int. Ed.*, 2009, **48**, 500.
- (a) G. Y. Wang, L. L. Yang, Y. Li, H. Song, W. J. Ruan, Z. Chang and X. H. Bu, *Dalton Trans.*, 2013, **42**, 12865; (b) H. Sohn, M. J. Sailor, D. Magde and W. C. Troglor, *J. Am. Chem. Soc.*, 2003, **125**, 3821.
- (a) B. L. Chen, Y. Yang, F. Zapata, G. Lin, Qian G., E. B. Lobkovsky, *Adv. Mater.*, 2007, **19**, 1693; (b) S. Dang, X. Min, W. T.

Yang, F. Y. Yi, H. P. You and Z. M. Sun, *Chem.-Eur. J.*, 2013, **19**, 17172.

Graphical Abstract

Three new solvent-directed Cd(II)-based MOFs with unique luminescent properties and highly selective sensor for Cu²⁺ cations and nitrobenzene

Yunlong Wu, Guo-Ping Yang*, Yanqing Zhao, Wei-Ping Wu, Bo Liu, Yao-Yu Wang*

Three new solvent-directed MOFs were yielded in different solvent systems. The luminescent properties of the MOFs were studied by UV light at ambient temperature, especially for **3** showing a highly selective sensitivity for sensing Cu²⁺ ions and NB molecules.

